The NOSA-ITACA code for the safety assessment of ancient constructions: a case study in Livorno

M. Girardi, C. Padovani and D. Pellegrini
Institute of Information Science and Technologies, Italian National Research Council, Pisa, Italy

Abstract

The present paper describes the main features of the finite element code NOSA-ITACA for the static and dynamic analysis of masonry buildings of historical interest. The code, which models masonry as a nonlinear elastic material with zero tensile strength and bounded compressive strength, is aimed at assessing the static safety and seismic vulnerability of masonry constructions in light of Italian regulations, as well as modelling possible strengthening interventions.
The NOSA-ITACA code has been used to study the "Voltone", a large vaulted masonry structure located beneath the "Piazza della Repubblica" square in Livorno. The structure has been analysed in the presence of permanent and accidental loads, calculated on the basis of current Italian regulations. This case study has provided the opportunity to validate the NOSA-ITACA code and highlighted the key role played by numerical tools in assessing the safety of ancient masonry constructions.

Keywords: masonry buildings, nonlinear elasticity, static analysis, numerical methods.

1 Introduction

Since the early 1900s awareness has been steadily growing of the incommensurable social and cultural value of the world's cultural heritage, as has the conviction that such heritage is the birthright of all people of the world. This has prompted both local and national authorities and administrations to take cultural heritage into account in their operating plans, with the aim of making it accessible to all citizens.
Article 2 of the Venice Charter [1] reads "The conservation and restoration of monuments must have recourse to all the sciences and techniques which can

contribute to the study and safeguarding of the architectural heritage". In recent years, according to the inspiring principle of article 2, the structural analysis of historical masonry buildings made possible by innovative mathematical models and computer technologies has gained increasing importance in safeguarding the world's architectural heritage.

In Italy many historically and artistically important masonry buildings are in dire need of maintenance and restoration. In order to optimize such operations in terms of cost-effectiveness, architectural impact and static effectiveness, numerical codes have a crucial role to play in modelling the structural behaviour of masonry buildings. By providing important information, such as the collapse loads, the stress field and the distribution of cracked regions, together with their possible evolution, such codes represent a valuable support in the choice and design of strengthening and seismic retrofitting operations.

For these reasons, it is crucial to realistically model masonry materials, whose response to tension is fundamentally different from that to compression, and whose mechanical properties depend on their constituent elements and the building techniques used. The numerous techniques proposed for modelling masonry structures can be grouped into the following main classes: micro–mechanical approaches [2], [3], rigid block modelling for limit analysis [4], [5] and dynamic analysis [6], homogenisation techniques [7], [8] and continuum models [9], [10], [11], [12]. The most common constitutive models used are the linear elastic [9]-[11] and the elastic-plastic model [2], [3], [6], [8] and [12]. The former provides only qualitative information on the global behaviour of masonry structures without however considering their inability to withstand tension, while the latter instead takes into account the strong nonlinearities of such structures' static and dynamic responses.

The studies described in [13] have led to the implementation of the finite element code NOSA, in which masonry is described as a nonlinear elastic material with zero tensile strength and bounded compressive strength. The code has been successfully applied to a number of studies, commissioned by both private and public bodies, on important historic buildings, such as the chimney of the Vecchi Macelli, the Medici Arsenal [13] and the church of San Pietro in Vinculis in Pisa [13], the San Nicolò Motherhouse in Noto, the Goldoni Theatre in Livorno, the Baptistery of the Volterra Cathedral, the bell tower of Buti [14], the church of Santa Maria Maddalena in Morano Calabro [13], the church of San Ponziano [15], the Torre delle Ore (Clock Tower) in Lucca, and the Rognosa tower in San Gimignano [16], [17].

In many cases, such studies have also provided important information on the structure's seismic vulnerability, which can be assessed with respect to current Italian and European regulations. Moreover, the effects of thermal variations and the effectiveness of various strengthening interventions, such as the application of chains, rods and retaining structures, can be evaluated, and those with the least environmental and visual impact identified.

With the aim of improving the performance of the NOSA code and equipping it with an interactive graphic tool for pre- and post-processing, the project "Tools for the modelling and assessment of the structural behaviour of ancient constructions" was conducted by the laboratory of Mechanics of Materials and Structures of ISTI-CNR

and a research team from the Department of Civil and Environmental Engineering of the University of Florence. The project [18], funded by the Region of Tuscany (2011-2013), was divided into two parts: research activity aimed at studying mathematical models for the static and dynamic behaviour of masonry constructions and procedures for assessing their static safety and seismic vulnerability, and the development of the NOSA-ITACA code, resulting from integration of the NOSA code and the open source graphic platform SALOME [19]. SALOME is used both to define the geometry of the structure under examination and to visualise the results of the structural analysis.
In this paper we present a study of the "Voltone" − a large vaulted masonry structure located beneath the Piazza della Repubblica square in Livorno, Italy. Section 2 is devoted to a general description of the NOSA-ITACA code and the mathematical models and numerical methods used for simulating the mechanical behaviour of masonry constructions. In section 3 a nonlinear structural analysis of the "Voltone" is presented, in which the safety of the structure is assessed under gravity and accidental loads. The most widely adopted assessment procedures for masonry bridges and tunnels are based on limit analysis and aim to estimate their load-bearing capacity [5], [20]-[24]. Instead, the study presented here follows a nonlinear incremental approach. This case study, conducted in collaboration with the Municipality of Livorno, has provided an opportunity to validate both the models proposed and the calculation tool developed, and constituted a pilot project for broader initiatives aimed at safeguarding Tuscany's cultural heritage.

2 The NOSA-ITACA code and the numerical modelling of masonry-like solids

2.1 The finite element code NOSA-ITACA

NOSA-ITACA is freeware/open-source software for computational mechanics, as is the Salome-Meca - Code_Aster package [25], and is distributed with the aim of disseminating the use of mathematical models and numerical tools in the field of Cultural Heritage. NOSA-ITACA is the result of the integration of the finite element code NOSA [13] into the open-source SALOME platform [19].
The finite element code NOSA (NOn-Linear Structural Analysis) has been developed by the Mechanics of Materials and Structures Laboratory of the ISTI-CNR with the aim of testing new constitutive models for materials. It has moreover been applied to checking the algorithms for integrating the equations of motion, as well as to other numerical techniques for solving structural engineering problems. The development of NOSA began in 1980 and has continued over the ensuing years along the research lines of the Lab.
The first version of the code included plane, three-dimensional and axisymmetric isoparametric elements [26] and allowed for elastic and elastic-plastic analyses in the presence of infinitesimal strains with the work-hardening models described in [27]. The code has subsequently been extended to include cases of finite strains and contact problems, based on studies performed on both the constitutive equations

[28]-[31] and the methods for numerical integration of the equations of motion, in the presence of follower forces [32], [33].
Over recent decades, constitutive models and calculation techniques have become available that enable realistic description of the static behaviour of masonry structures. Several studies [34], [35], [13] have led to a better understanding of the constitutive equation of materials not withstanding tension, known in the literature as *masonry-like* or *no-tension* materials. Within this framework, masonry is modelled as a nonlinear elastic material, with zero tensile strength and infinite or bounded compressive strength.
In order to study real problems, the equilibrium problem of masonry structures can be solved via the finite element method. To this end, suitable numerical techniques have been developed [13] based on the Newton-Raphson method for solving the nonlinear system obtained by discretising the structure into finite elements. Their application requires that the derivative of the stress with respect to the strain be explicitly known, as this is needed in order to calculate the tangent stiffness matrix. The numerical method studied has therefore been implemented into the NOSA code to enable determination of the stress state and the presence of any cracking. It can moreover be applied to modelling needed restoration and reinforcement operations on constructions of particular architectural interest.
The code has been further enhanced to enable performing nonlinear heat-conduction analysis on solids even in the non-stationary case, with boundary conditions concerning temperature and thermal fluxes. Today, the code provides for thermo-mechanical analysis of no-tension solids whose mechanical characteristics depend on temperature in the presence of thermal loads [36], [37].
Finally, numerical solution of dynamic problems requires direct integration of the equations of motion [38]. In fact, due to the nonlinearity of the adopted constitutive equation, the mode-superposition method is meaningless. With an aim to solving such problems, we have instead implemented the Newmark [39] method within NOSA in order to perform the integration with respect to time of the system of ordinary differential equations obtained by discretising the structure into finite elements. Moreover, the Newton-Raphson scheme, needed to solve the nonlinear algebraic system obtained at each time step, has been adapted to the dynamic case.
The code has been successfully applied to the analysis of arches and vaults [40], as well as some buildings of historical and architectural interest [13], [14], [16], [17].
Development of the code has been made possible through the funding of the CNR, the Italian Ministry of Universities and Research and the region of Tuscany (NOSA-ITACA project).
Within the framework of this project, the NOSA code has been substantially modified and significantly improved in light of FORTRAN 90 specifications and equipped with new finite elements, thus enhancing its application capabilities. An efficient implementation of numerical methods for constrained eigenvalue problems for the special case of modal structural analysis taking into account both the sparsity of the matrices and the features of master-slave constraints (tying or multipoint constraints) has been embedded in NOSA. Such implementation is based on the open-source packages SPARSKIT [41], for managing matrices in sparse format (storage, matrix-vector products), and ARPACK [42], which implements a method

based on the Lanczos factorization combined with spectral techniques that improve convergence.
Implementation of the NOSA-ITACA code for the structural analysis of historical masonry constructions was then completed by integrating the finite element code NOSA within the open-source interactive graphic code SALOME [19]. Specifically, the NOSA code has been implemented within the SALOME architecture (developed mostly in the C/C++ and Python languages) as an additional module on a par with those already existing (MESH, GEOM, POST-PRO). Through such integration the NOSA module thus allows the user to define the physical quantities to associate to a mesh (materials, element thickness, boundary conditions, loads, analysis type, etc.), display the load applied to the structure, generate the input file for running and monitoring the finite element analysis, etc. Moreover, the NOSA module allows the user to monitor the analysis and transmits the results of the numerical study to the POST-PRO module.
Recent applications of the NOSA-ITACA code are described in [43]-[47]. In particular, comparative dynamic analyses of masonry towers conducted via the NOSA-ITACA and MADY [48] codes are presented in [44], while [45], [46] and [47] provide descriptions of a preliminary study of the "Voltone" and the church of San Francesco in Lucca.

2.2 The constitutive equation of masonry-like materials

In order to model the structural behaviour of masonry constructions, we have adopted the constitutive equation of masonry-like materials described in [13]. Masonry is assumed to be a nonlinear hyperelastic material with zero tensile strength and finite compressive strength. Despite its simplicity, this constitutive equation enables modelling the most important aspects of the mechanical behaviour of masonry constructions, which are due to their different behaviour under tensile and compressive stresses. The masonry-like material is characterized by the Young's modulus $E > 0$, Poisson's ratio ν with $0 \le \nu < 1/2$ and a compressive strength, $\sigma_0 < 0$.
The masonry-like constitutive equation is described in the following. Let us denote by *Sym* the vector space of symmetric tensors with the inner product $\mathbf{A} \cdot \mathbf{B} = tr(\mathbf{AB})$, $\mathbf{A}, \mathbf{B} \in Sym$ and *tr* the trace. Let Sym^- and Sym^+ be the cones of *Sym* constituted by the negative and positive semidefinite tensors, respectively. We assume that the infinitesimal strain $\mathbf{E} \in Sym$ is the sum of an elastic part $\mathbf{E}^e \in Sym$ and two mutually orthogonal inelastic parts $\mathbf{E}^f \in Sym^+$ and $\mathbf{E}^c \in Sym^-$, respectively called fracture strain and crushing strain,

$$\mathbf{E} = \mathbf{E}^e + \mathbf{E}^f + \mathbf{E}^c, \ \mathbf{E}^f \cdot \mathbf{E}^c = 0, \tag{1}$$

and that the Cauchy stress **T** depends linearly and isotropically on $\mathbf{E}^e$,

$$\mathbf{T} = \frac{E}{1+\nu}[\mathbf{E}^e + \frac{\nu}{1-2\nu} tr(\mathbf{E}^e)\mathbf{I}]. \quad (2)$$

Lastly, we assume that $\mathbf{T}$, $\mathbf{E}^f$ and $\mathbf{E}^c$ satisfy the conditions

$$\mathbf{T} \in Sym^-, \quad \mathbf{T} - \sigma_0 \mathbf{I} \in Sym^+, \quad (3)$$

and

$$\mathbf{E}^f \cdot \mathbf{T} = (\mathbf{T} - \sigma_0 \mathbf{I}) \cdot \mathbf{E}^c = 0, \quad (4)$$

with $\mathbf{I} \in Sym$ the identity tensor, meaning that the material does not dissipate energy while crushing and cracking. For σ_0 tending towards $-\infty$ the constitutive equation (1)-(4) conforms to the more classical equation of masonry-like materials with infinite compressive strength dealt with in [34] and [35].

The stress tensor $\mathbf{T}$ satisfying the constitutive equation (1)-(4) can be expressed as a nonlinear function of the total strain $\mathbf{E}$, $\mathbf{T} = \hat{\mathbf{T}}(\mathbf{E})$ by using the coaxiality of $\mathbf{E}$, $\mathbf{T}$, $\mathbf{E}^f$ and $\mathbf{E}^c$. Both $\hat{\mathbf{T}}$ and its derivative $D_E\hat{\mathbf{T}}(\mathbf{E})$ with respect to $\mathbf{E}$, necessary to build the tangent stiffness matrix, have been explicitly calculated in [13] for three- and two-dimensional cases.

Here we recall how this constitutive equation can be applied to the study of masonry shell structures such as vaults, domes, arches etc, by using thick shell elements [49] based on Mindlin plate theory [50].

Formulation of the element, a four-node quadrilateral with six degrees of freedom per node, is based on the following hypotheses: (i) displacements and strain are infinitesimal, (ii) the unit vector $\mathbf{n}$ orthogonal to the mean surface of the shell maintains its length after deformation.

Now let η_1 and η_2 be an orthogonal coordinate system defined on the mean surface Σ of the element of thickness h shown in Figure 1, with $\zeta \in [-h/2, h/2]$ as the coordinate in the normal direction $\mathbf{n}$. We denote by $\mathbf{g}_1$ and $\mathbf{g}_2$ the unit tangent vectors to the η_1 and η_2 axis, respectively.

The structure can be considered to be made up of the layers

$$\Sigma_\zeta = \{\mathbf{p}' = \mathbf{p} + \zeta\, \mathbf{n}, \;\; \mathbf{p} \in \Sigma, \; \mathbf{n} = \mathbf{n}(\mathbf{p})\}, \quad \zeta \in [-h/2, h/2], \quad (5)$$

and strain tensor $\mathbf{E}$ and stress tensor $\mathbf{T}$ are functions of $\mathbf{p}$ and ζ.

We denote by $E_{ij} = \mathbf{g}_i \cdot \mathbf{E}\, \mathbf{g}_j$, $T_{ij} = \mathbf{g}_i \cdot \mathbf{T}\mathbf{g}_j$ $i, j = 1, 2, 3$, the components of $\mathbf{E}$ and $\mathbf{T}$ with respect to the orthonormal basis $\{\mathbf{g}_1, \mathbf{g}_2, \mathbf{g}_3\}$, with $\mathbf{g}_3 = \mathbf{n}$. Hypothesis (ii) implies that there are no changes in thickness, namely $E_{33} = 0$, and the transverse shear strains E_{13} and E_{23} are thereby constant along the thickness.

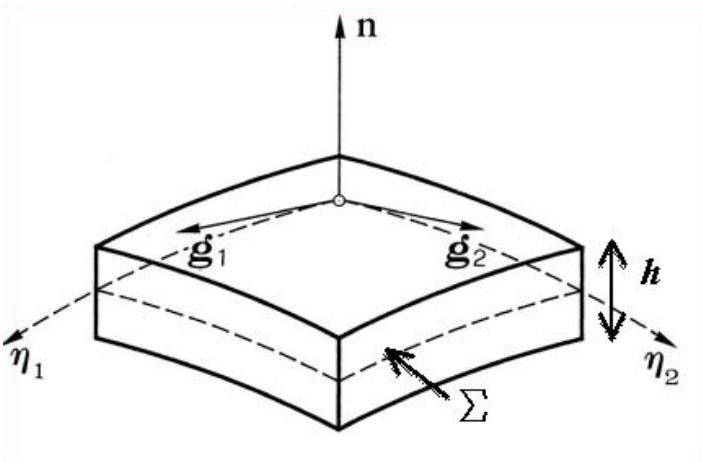

Figure 1: Shell element.

The displacements and rotations within the element are given by the relations $\mathbf{u} = \sum_{i=1}^{4} \varphi_i \mathbf{u}_i$, $\boldsymbol{\theta} = \sum_{i=1}^{4} \varphi_i \boldsymbol{\theta}_i$, where $\mathbf{u}_i$ and $\boldsymbol{\theta}_i$ are respectively the displacement vector and the rotation of the i-th node, and φ_i, i =1,. . . , 4 are bilinear shape functions. The vector of infinitesimal strains $\boldsymbol{\varepsilon} = (E_{11}, E_{22}, E_{12}, E_{13}, E_{23})^T$ can be expressed as a function of the generalized displacements $\tilde{\mathbf{u}} = (\mathbf{u}_1, \boldsymbol{\theta}_1, \mathbf{u}_2, \boldsymbol{\theta}_2, \mathbf{u}_3, \boldsymbol{\theta}_3, \mathbf{u}_4, \boldsymbol{\theta}_4)^T$ via the matrix B containing the derivatives of the shape functions φ_i, $\boldsymbol{\varepsilon} = \mathbf{B}\,\tilde{\mathbf{u}}$. In particular, matrix B can be written as

$$\mathbf{B} = \mathbf{B}^m + \zeta\, \mathbf{B}^\theta , \tag{6}$$

where matrices $\mathbf{B}^m$ and $\mathbf{B}^\theta$ take into account the membrane strains and the curvature variations, respectively. The elemental tangent stiffness matrix is

$$\mathbf{K}_T = \int_A \int_{-h/2}^{h/2} \mathbf{B}^T D_E \hat{\mathbf{T}}\, \mathbf{B}\, \mathrm{d}\zeta\, \mathrm{dA} , \tag{7}$$

where A is the area of the element and $D_E \hat{\mathbf{T}}$ is the derivative of the stress function $\hat{\mathbf{T}}$ with respect to strain. In view of (6), for $\mathbf{D} = D_E \hat{\mathbf{T}}$, omitting simple calculations, relation (7) becomes

$$\mathbf{K}_T = \int_A \begin{bmatrix} \mathbf{B}^{mT} & \mathbf{B}^{\theta T} \end{bmatrix} \begin{bmatrix} \mathbf{D}_0 & \mathbf{D}_1 \\ \mathbf{D}_1 & \mathbf{D}_2 \end{bmatrix} \begin{bmatrix} \mathbf{B}^m \\ \mathbf{B}^\theta \end{bmatrix} \mathrm{dA} , \tag{8}$$

where

$$\mathbf{D}_0 = \int_{-h/2}^{h/2} \mathbf{D}\, \mathrm{d}\zeta , \qquad \mathbf{D}_1 = \int_{-h/2}^{h/2} \zeta\, \mathbf{D}\, \mathrm{d}\zeta , \qquad \mathbf{D}_2 = \int_{-h/2}^{h/2} \zeta^2\, \mathbf{D}\, \mathrm{d}\zeta . \tag{9}$$

We denote by $E_{ij}^f = \mathbf{g}_i \cdot \mathbf{E}^f \mathbf{g}_j$ and $E_{ij}^c = \mathbf{g}_i \cdot \mathbf{E}^c \mathbf{g}_j$, $i, j = 1, 2$ the components of $\mathbf{E}^f$, and $\mathbf{E}^c$ with respect to $\mathbf{g}_1$ and $\mathbf{g}_2$. The quantities $N_i(\mathbf{p}) = \int_{-h/2}^{h/2} T_{ii}(\mathbf{p}, \zeta) d\zeta$ and

$M_i(\mathbf{p}) = \int_{-h/2}^{h/2} T_{ii}(\mathbf{p},\zeta)\zeta \, d\zeta$ for $i = 1, 2$ are the normal force and bending moment (per unit length) at point **p** of the mean surface Σ. The ratios

$$e_i(\mathbf{p}) = \frac{M_i(\mathbf{p})}{N_i(\mathbf{p})} \tag{10}$$

are the eccentricities at $\mathbf{p} \in \Sigma$ along $\mathbf{g}_i$, $i = 1, 2$. Moreover, by considering the limited compressive strength σ_0, we have [51]

$$-\frac{h}{2}\left(1 - \frac{N_i}{N_0}\right) \le e_i(\mathbf{p}) \le \frac{h}{2}\left(1 - \frac{N_i}{N_0}\right), \qquad \text{for each } \mathbf{p} \in \Sigma, \tag{11}$$

with $N_0 = \sigma_0 h$.

3 Case study: the "Voltone" in Livorno, Italy

The "Voltone" (i.e., the great vault) is a 220-meter long, tunnel-like masonry structure located beneath Piazza della Repubblica in Livorno (Figures 2, 3 and 4). It is constituted by a segmental vault, through which the "Fosso Reale" canal flows. The vault is set on two lateral walls and strengthened by buttresses placed at intervals of about 5.8 meters one from the other.

Figure 2: *Piazza della Repubblica* square and the "Voltone", northern side.

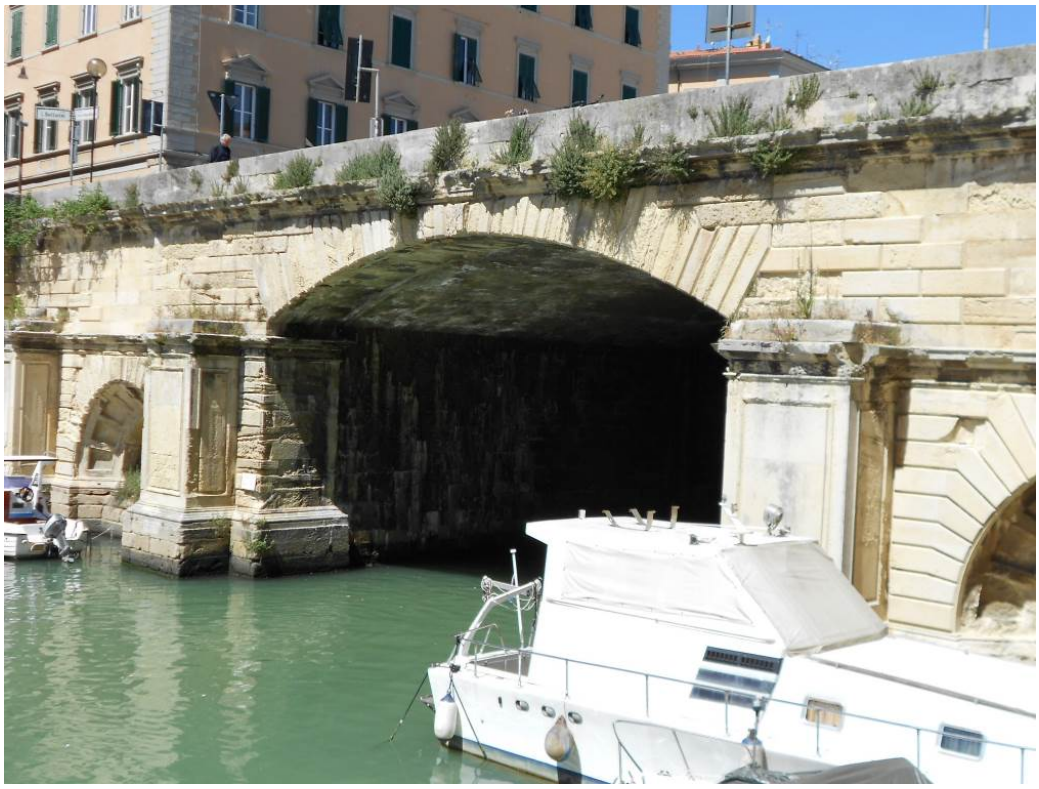

Figure 3: The “Voltone”, southern side.

In order to realistically model the structural behaviour of this monument via a finite element code, the geometry, the mechanical properties of the constituent materials, and the characteristics of the soil and surrounding structures are needed. The permanent and accidental loads acting on the structure must moreover be assessed as well. To this end, some non-destructive tests were conducted (laser scan digital acquisition and georadar scan of the surface of the tunnel and overlying square), and four vertical core samples extracted, two from the wall and surrounding soil, and two from the vault (at the crown and haunch), with the aim of accurately measuring the thickness of the vault and walls and determining the stratigraphy and mechanical properties of their constituent materials. In addition, two horizontal core samples were extracted from the lateral walls, starting from the intrados. The results of these tests were then supplemented by data gathered from historical and archaeological reports [52]. The information collected allowed us to build a three-dimensional finite element model (Figures 5 and 6), which has been used to verify the static conditions of the structure. The model was built by collecting 43228 thick shell and beam elements (elements 9 and 10 of the NOSA-ITACA library [53]) and 45379 nodes; the connections between the vault and the lateral wall elements were guaranteed by multipoint constraints able to model the geometrical misalignment between the vault and the wall, and specified by expressly developed user routine*s* [53].

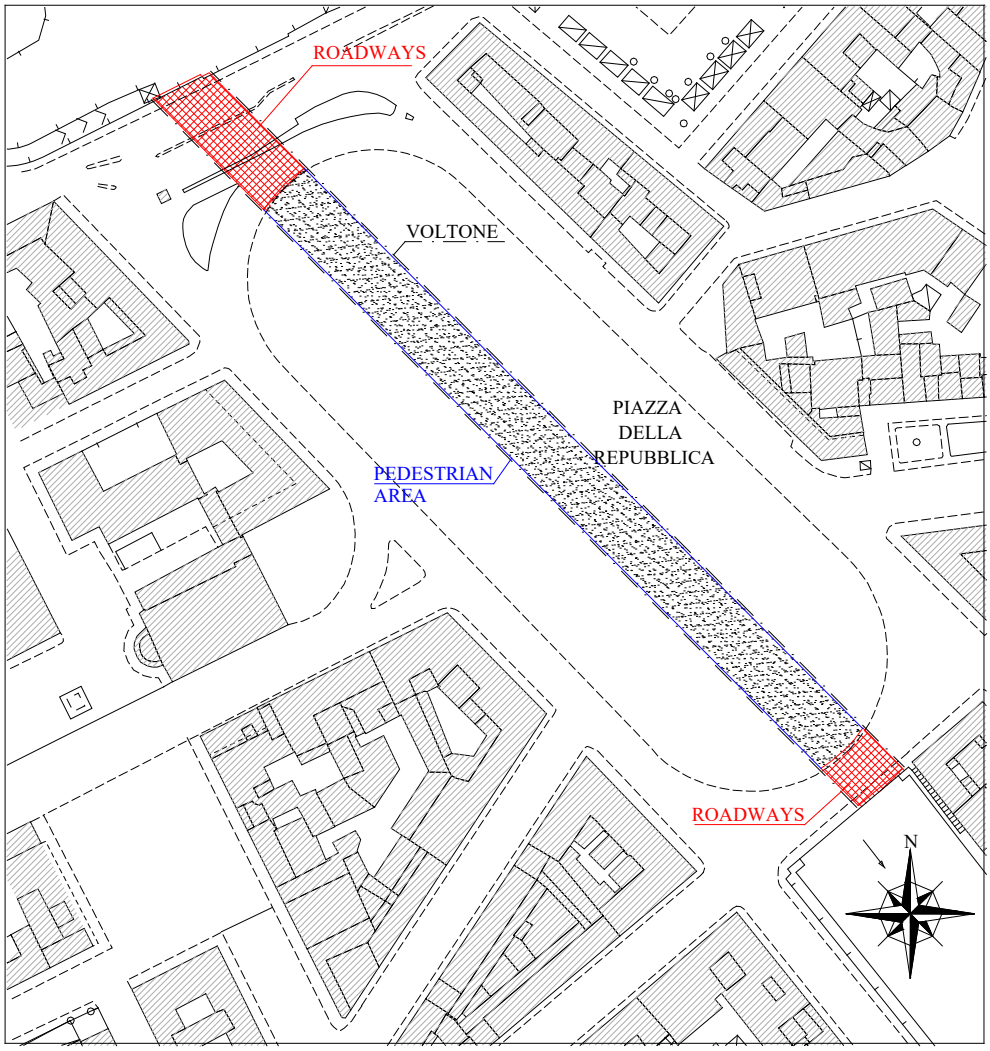

Figure 4: Map of *Piazza della Repubblica* square.

The vault, made of lime mortar and bricks, is about 0.41÷0.43 m thick, with constant thickness along the section and length of the vault, except for the tunnel's ends (in correspondence to the roadways, see Figure 4), where the thickness increases to about 0.7 m. The vault's structure, which is segmental (quite 'lowered' with respect to a semicircle), spans 12.4 m and has a rise of about 1.65 m.
The lateral walls, made up by external layers of a local chalky stone and an inner cohesive mortar core layer, are variable in height above the surface of the canal, decreasing from 5.27 m to 2.65 m. The walls' maximum overall height is 9.3 m with a thickness of about 2.3 m. According to [52], the walls have been strengthened by some buttresses, whose thickness has been set to 1.6 m. Table 1 lists the mechanical properties chosen for each structural element, as deduced by laboratory tests on the material extracted and according to [54], [55]. The weight of the structure has been calculated assuming 1800 daN/m^3 for the vault and 2000 daN/m^3 for the lateral walls with buttresses.

Element	Young modulus E [daN/m^2]	Shear strength τ_c [daN/m^2]	Compressive strength $\|\sigma_c\|$ [daN/m^2]	Partial factor for the material γ_m	Design compressive strength $\|\sigma_0\|$ [daN/m^2]
Vault	$1.5\text{x}10^8$	17100	720000	3.0	240000
Lateral walls	$1.23\text{x}10^8$	9700	562500	3.0	187500
Buttresses	$1.23\text{x}10^8$	9700	562500	3.0	187500

Table 1- Mechanical properties of the model's structural elements

A number of relevant scientific papers addressing the structural behaviour of masonry bridges have been published in the international literature. The fundamental role played by the complex interactions between masonry and soil on the load capacity of such structures has been generally recognized. In particular, as shown in [5] and [20]-[24], the infill contributes significantly to the statics of masonry bridges, both by distributing the concentrated vertical loads induced by traffic and by restraining the horizontal displacements of the structure. In [20]-[22] the authors take these effects into account by directly modelling the soil via finite elements and interface elements at the juncture with the masonry structure. In [5], [23], [24] the infill is modelled via unilateral constraints able to develop a lateral reaction equivalent to the passive lateral earth pressure.

In the formulated model, the dispersion effect of the load through the fill has been taken into account by introducing an internal friction angle $\Phi = 31°$, while, due to the fact that the vault is segmental, the retaining effect of the soil surrounding the structure has been applied on the lateral walls only.

The permanent and accidental loads have been applied incrementally. With regard to the lateral earth pressure acting on the structure, an equivalent horizontal load has been considered as acting on the lateral walls and linearly variable along their height following classical Rankine theory. The coefficient k_0 [56] of the at rest lateral earth pressure has been considered for permanent loads, while for accidental loads, two limit situations have instead been considered: the first (Case 1) in which the lateral earth pressure values are maintained constant and equal to those calculated for permanent loads; and the second (Case 2) in which the lateral loads are increased incrementally together with the accidental loads until a lateral thrust value is attained corresponding to a coefficient of about 0.3 k_p, where k_p is the passive earth pressure coefficient given by Rankine limit theory [56], [57]. This reduced value is often employed in the literature [5] and seems to be reasonable, considering that the total value of the passive earth pressure coefficient k_p is activated only by very large deformations of the masonry-soil system. For an internal friction angle $\Phi = 31°$, and null cohesion, we have $k_0 = 1\text{-}\sin\Phi = 0.485$, $k_p = \text{tg}^2(45°+\Phi/2) = 3.11$.

With regard to accidental loads, their values were calculated in such a way as to match the structure's usage class according to Italian regulations [54], [55]. More precisely, under permanent loads, such as the weight of the structure and filling material and the earth pressure acting on the walls, two different types of accidental loads were considered: a load modelling the presence of a dense crowd of people (5

kN/m^2) in the central region of the square, and a traffic load for category II bridges at the square's ends, where roadways are located (Figures 7 and 8). According to [54], the traffic load is constituted by a distributed load and a set of concentrated loads applied on conventional lanes, as shown in Figure 8. The above loads were applied to the structure in accordance with the load combinations for ultimate limit states prescribed by Italian regulations [54], [55]. In order to simulate a live load, two different positions were considered along the vault's span to model an overload at the vault's crown and at its haunches.

The analyses have enabled calculating the stress, fracture and crushing strain fields and assessing the structure's safety (checks are being carried out in light of current Italian Regulations [54], [55]). The results are reported also in terms of line of thrust (Figures 9 and 10) through a diagram mapping function $e_i(\mathbf{p})$ defined in (10) on a given transverse section of the structure. Indeed, a line of thrust that is well contained within the thickness of the structure is an indication of static safety [4], [13], as also expressed by inequality (11).

Other safety checks aimed at studying the structure's behaviour at its ultimate limit states were easily implemented and tested in the NOSA-ITACA code. They are based on the partial factor method [54], formulated for checking the bending behaviour of the structure via the inequality

$$\left|\frac{M_i}{M_{iRd}}\right| \le 1, \tag{12}$$

where M_i is the bending moment per unit length defined in Section 2, and M_{Rd} is the corresponding ultimate limit moment per unit length (i.e. the maximum value of the bending moment that can be attained in the section), given, for a rectangular section, by the expression

$$M_{iRd} = \left(h^2 \frac{|\sigma_{im}|}{2}\right)\left(1 - \left|\frac{\sigma_{im}}{\sigma_0}\right|\right), \tag{13}$$

where σ_{im} is the mean value acting in the cross section due to the axial force N_i and σ_0 is the design compressive strength specified in Table 1.

Checks on the shear strength were based on the expression

$$\left|\frac{T_{ij}}{f_{ivd}}\right| \le 1, \tag{14}$$

where f_{ivd} is the limit tangential stress on the section of normal vector $\mathbf{g}_i$, (see Figure 6, with $\mathbf{g}_3 = \mathbf{n}$), as evaluated by the expression

$$f_{ivd} = (\tau_c + 0.4 \cdot |\sigma_{im}|) / \gamma_m, . \tag{15}$$

where τ_c is the shear strength specified in Table 1.

Figures 9 and 10 show the line of thrust for the load at the haunches and crown, respectively, for a transverse section at the southern end of the tunnel, where the structures reach the maximum lateral wall height. The line of thrust for permanent loads is shown in red, while the different accidental loads scenarios are represented by the green curve for Case 1, and the blue one for Case 2. In both figures, moving

from Case 1 to Case 2, the effects of the increased values of the lateral earth pressure are evident: the lateral wall eccentricity in Case 1 reaches the limit value expressed by (11). In Case 2 the eccentricity values tend to diminish along the walls, changing sign near the foundations. The presence of the filling, in terms of weight increase and concentrated loads distribution, helps the vault to contain the effects of the traffic loads. The eccentricity reaches its limit values in the vault under the concentrated loads and at the haunches. All Figures from 11 to 22 are relative to the traffic loads on the vault crown. In particular, Figures 11 to 14 show the vertical stresses at the intrados and extrados of the lateral walls plotted for Cases 1 and 2. The retaining effects of the lateral earth pressure are even more evident. Figures 15 and 16 show the fracture strains at the intrados of the tunnel for Cases 1 and 2, respectively. Figures 17 to 22 instead show ratios $\left|\frac{M_i}{M_{iRd}}\right|$ and $\left|\frac{T_{ij}}{f_{ivd}}\right|$ along the tunnel and in the buttresses for Cases 1 and 2. It is noteworthy that, while relation (12) is well satisfied along the entire structure, the shear checks (14) are not satisfied, and in both cases the tangential stresses reach very high values at the vault haunches, at the base of the lateral walls and in the buttresses. This situation, though limited to small portions of the structure and determined in part by the very low values of the shear strength specified by Italian Regulations, nonetheless requires monitoring. In particular, further tests should be planned to better define the geometry and mechanical characteristics of the buttresses, whose contribution is essential to the tunnel's static equilibrium. Moreover, in consideration of the high traffic volumes characterising "Piazza della Repubblica" square, structural monitoring of the traffic-induced vibrations is also highly advisable.

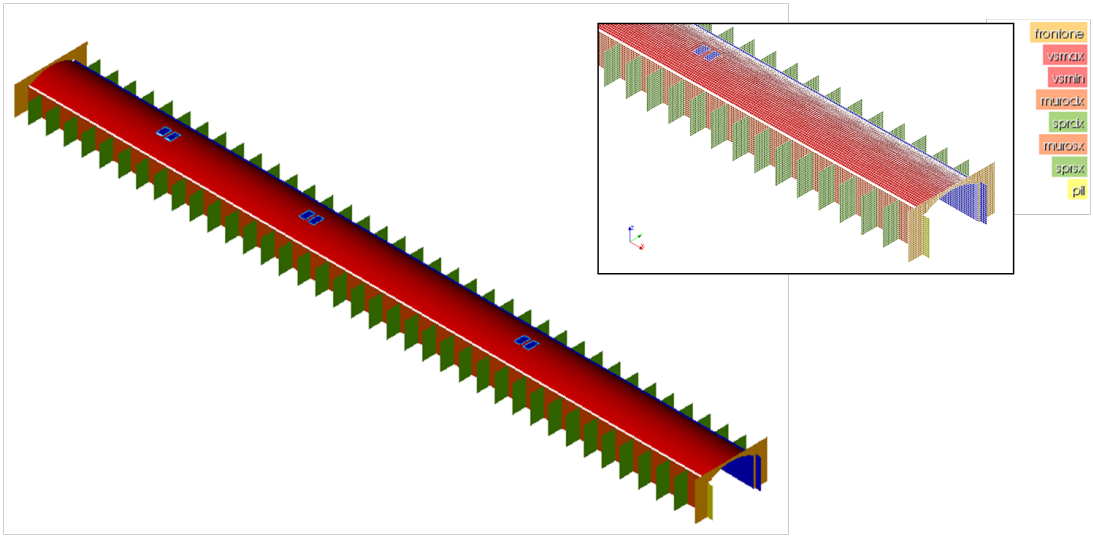

Figure 5: The finite element model built via the NOSA-ITACA code: overall view and detail (right).

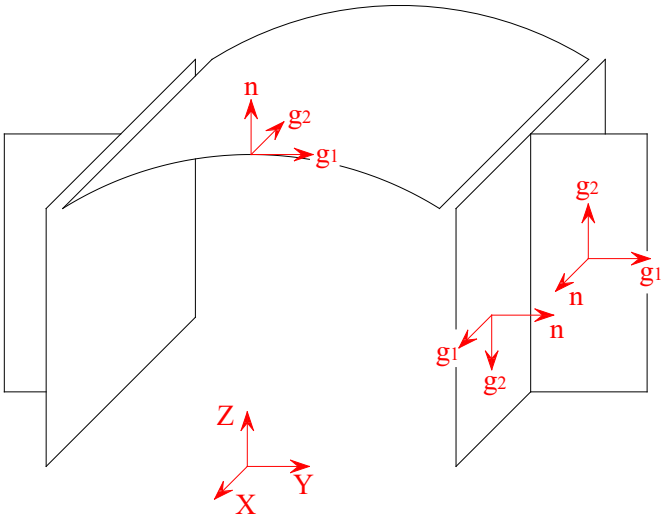

Figure 6: Definition of the local axes for the vault, walls and buttresses.

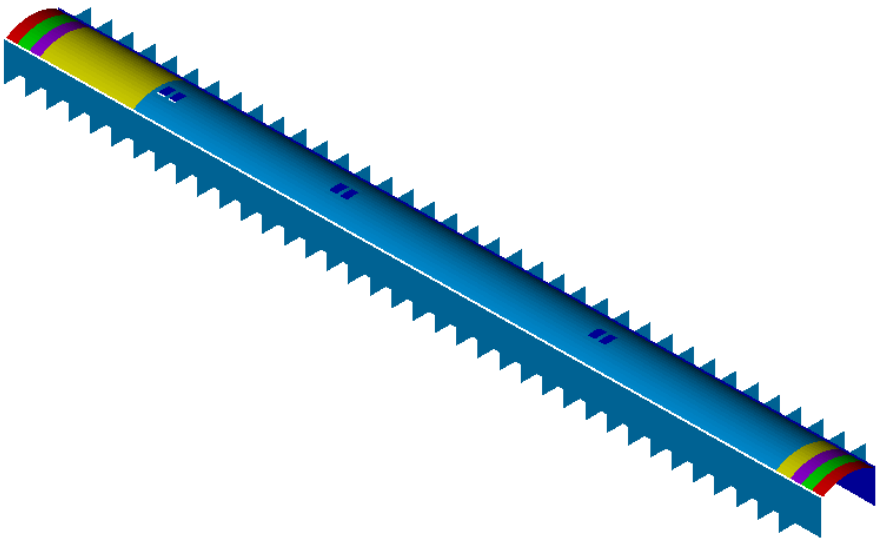

Figure 7: Map of the conventional lanes over the extrados of the tunnel: lane 1 in red, lane 2 in green, lane 3 in violet, other lanes in yellow.

Lanes	Axle load Q_{ik} [kN]	Distributed load q_{ik} [kN/m]
L1	240	7.20
L2	200	2.50
L3	100	2.50
L4	0.00	2.50

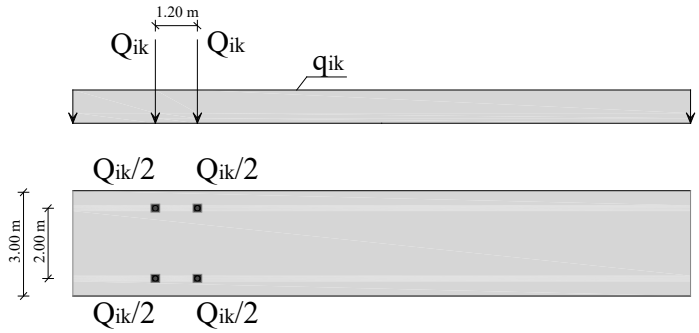

Figure 8: Scheme of the conventional traffic loads as defined in [54].

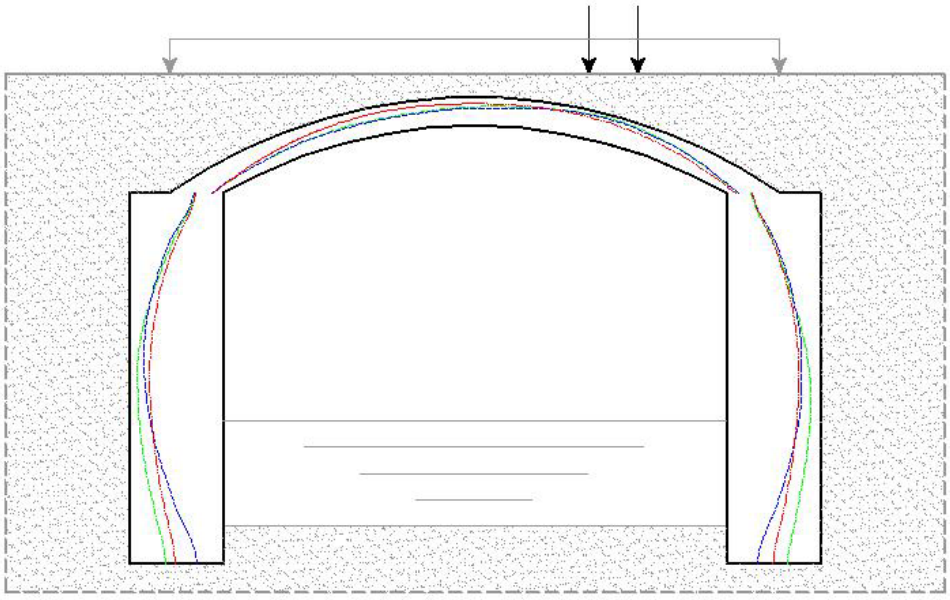

Figure 9: Southern side of the "Voltone": lines of thrust for permanent loads (red line) and traffic loads at the haunches for Case 1 (green) and Case 2 (blue).

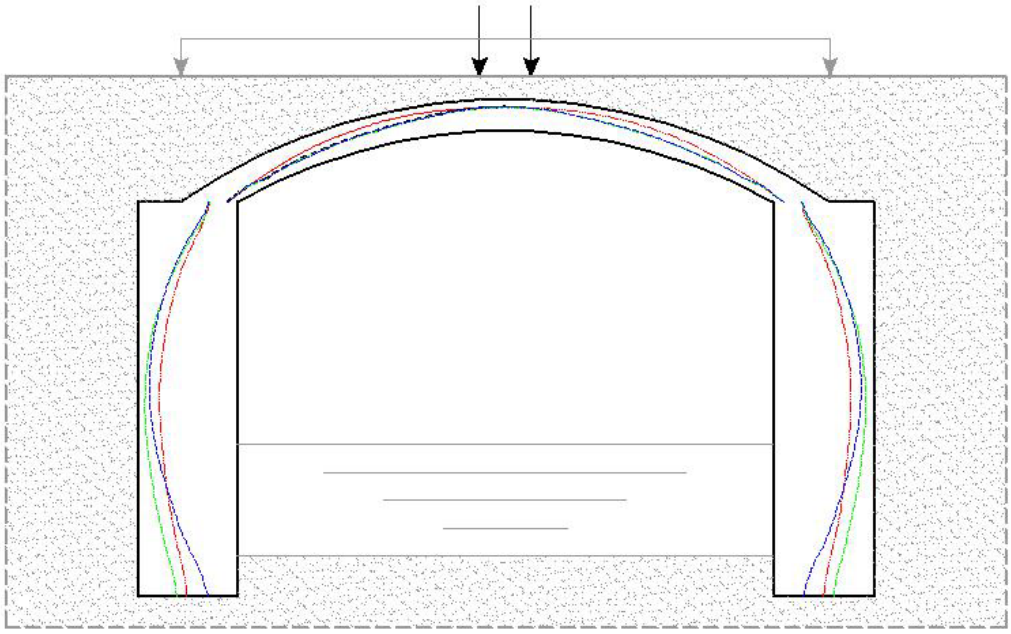

Figure 10: Southern side of the “Voltone”: lines of thrust for permanent loads (red line) and traffic loads at the arch crown for Case 1 (green) and Case 2 (blue).

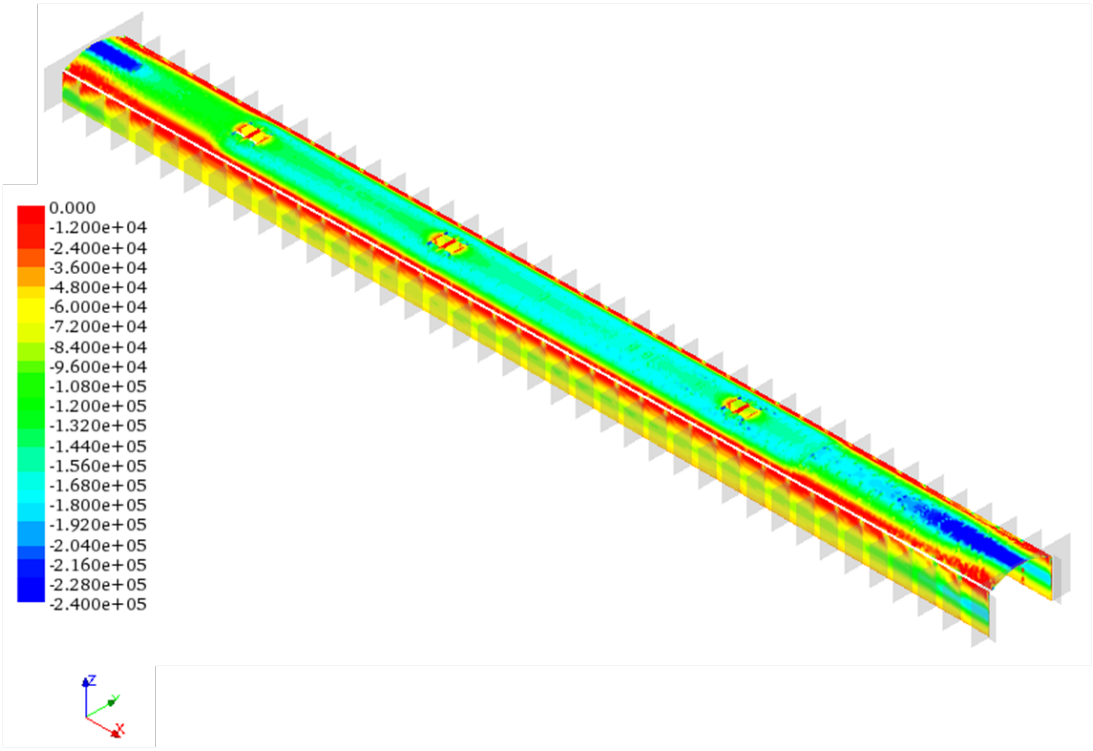

Figure 11: Case 1. Stresses T_{11} at the vault extrados and T_{22} at the extrados of the lateral walls.

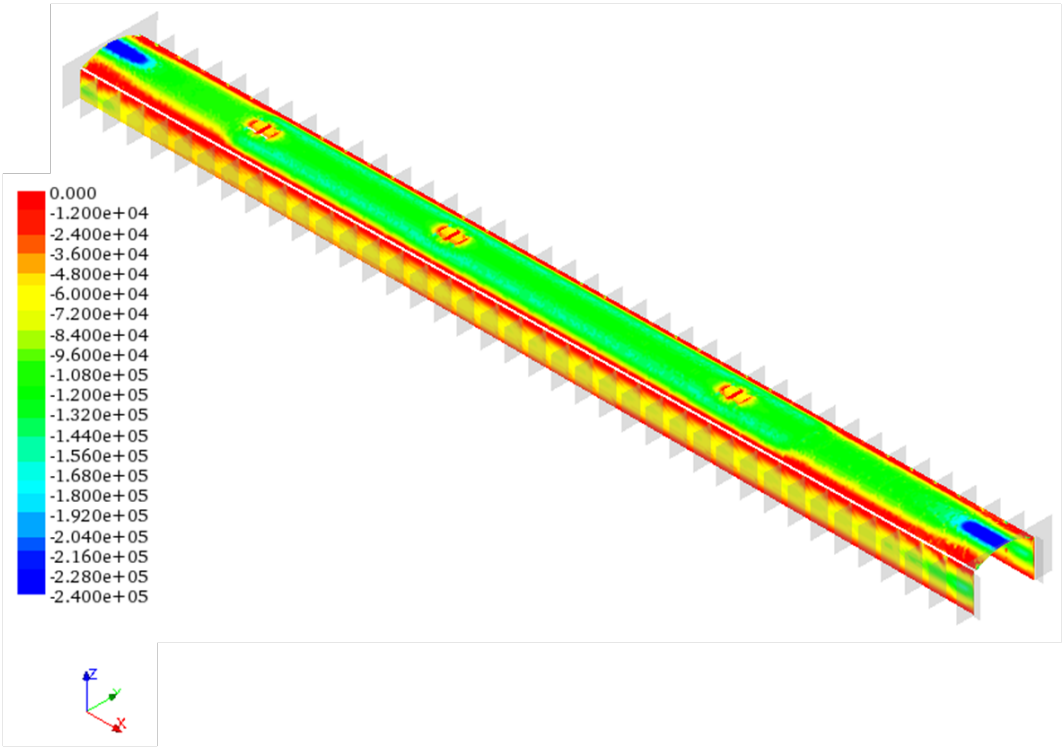

Figure 12: Case 2. Stresses T_{11} at the vault extrados and T_{22} at the extrados of the lateral walls.

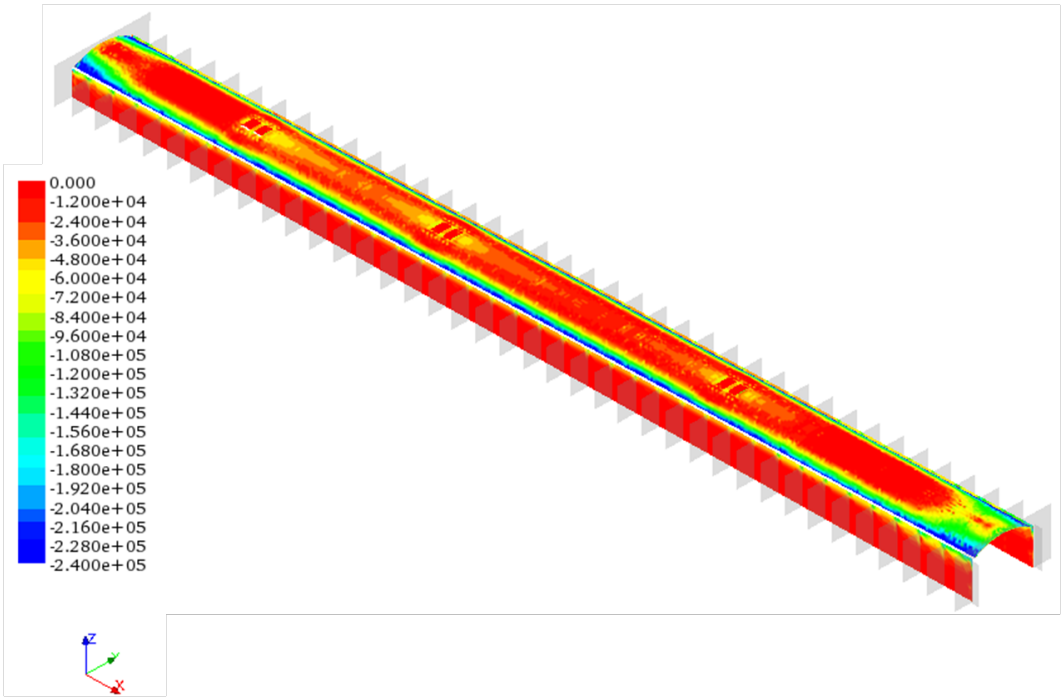

Figure 13: Case 1. Stresses T_{11} at the vault intrados and T_{22} at the intrados of the lateral walls.

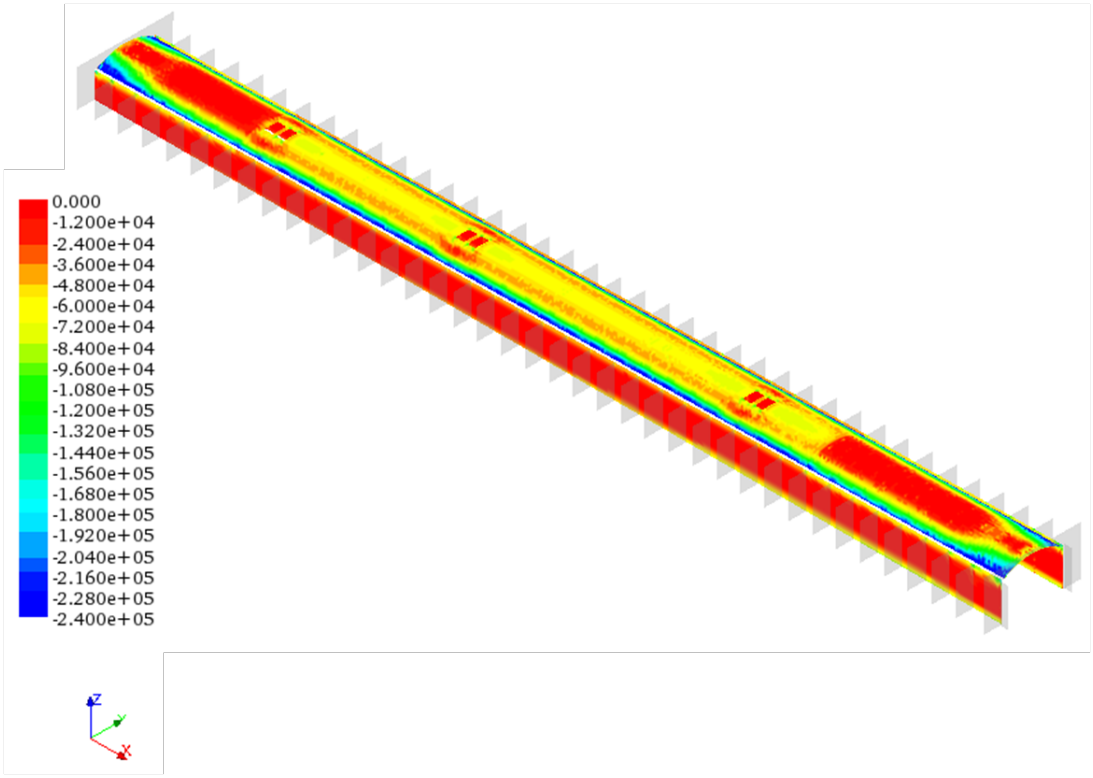

Figure 14: Case 2. Stresses T_{11} at the vault intrados and T_{22} at the intrados of the lateral walls.

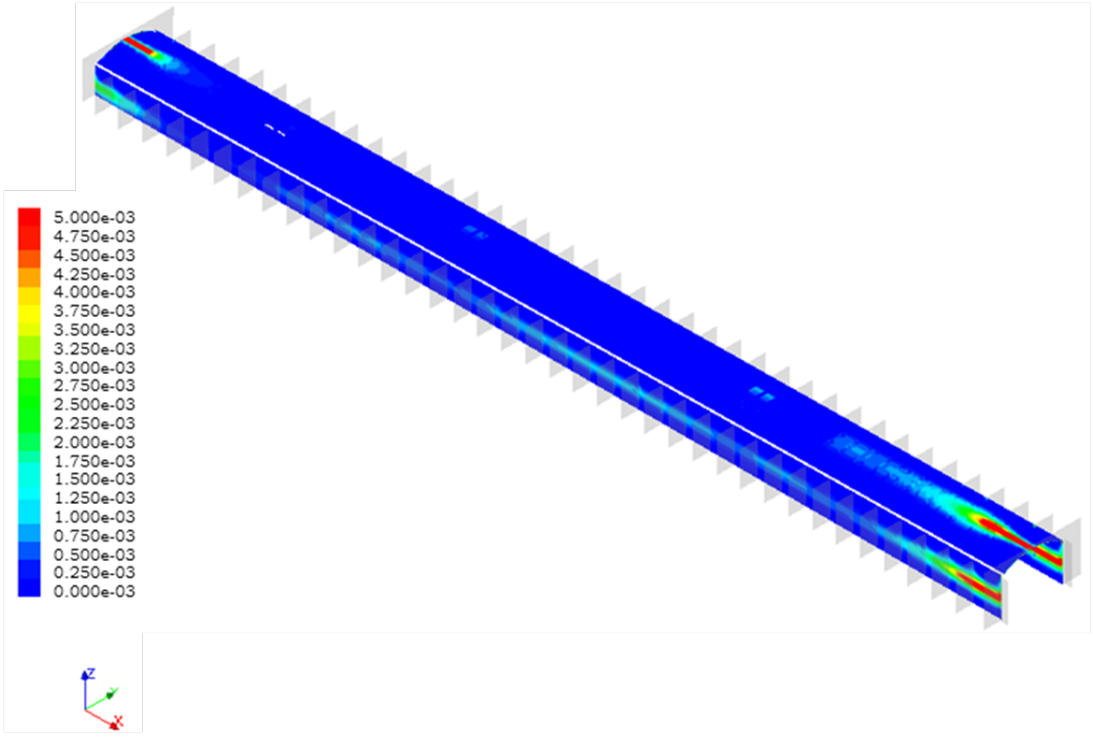

Figure 15: Case 1. Fracture strain E_{11}^f at the vault intrados and E_{22}^f at the intrados of the lateral walls.

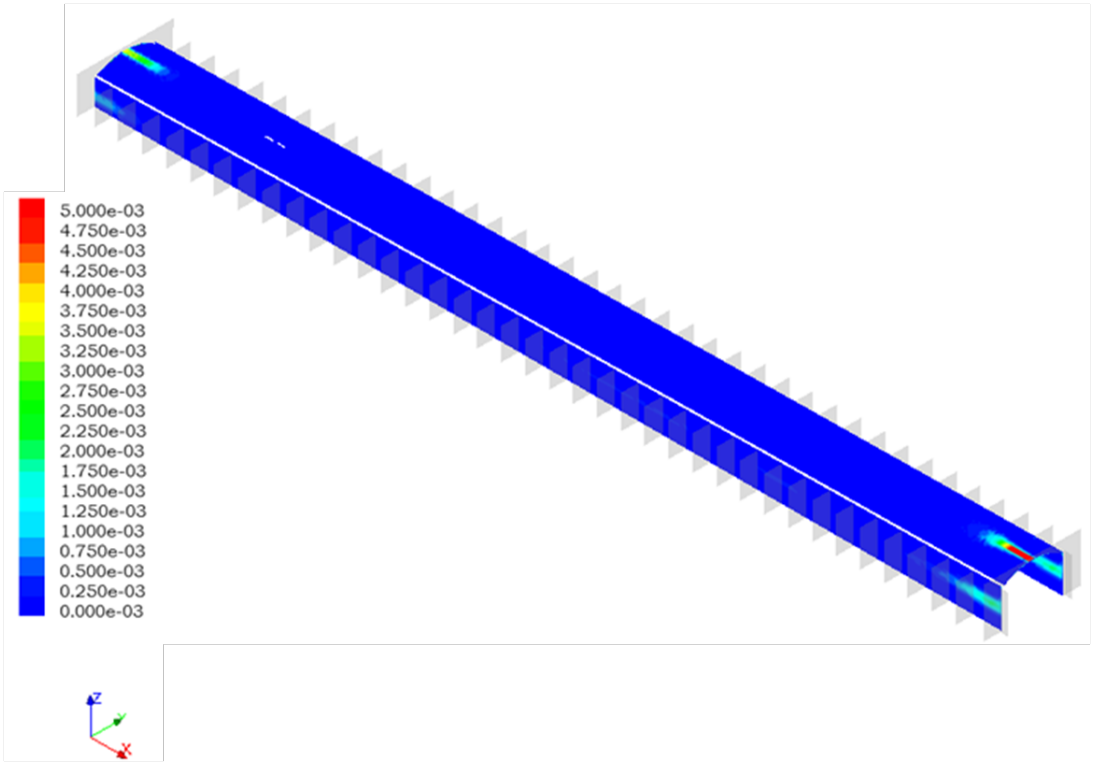

Figure 16: Case 2. Fracture strain E_{11}^{f} at the vault intrados and E_{22}^{f} at the intrados of the lateral walls.

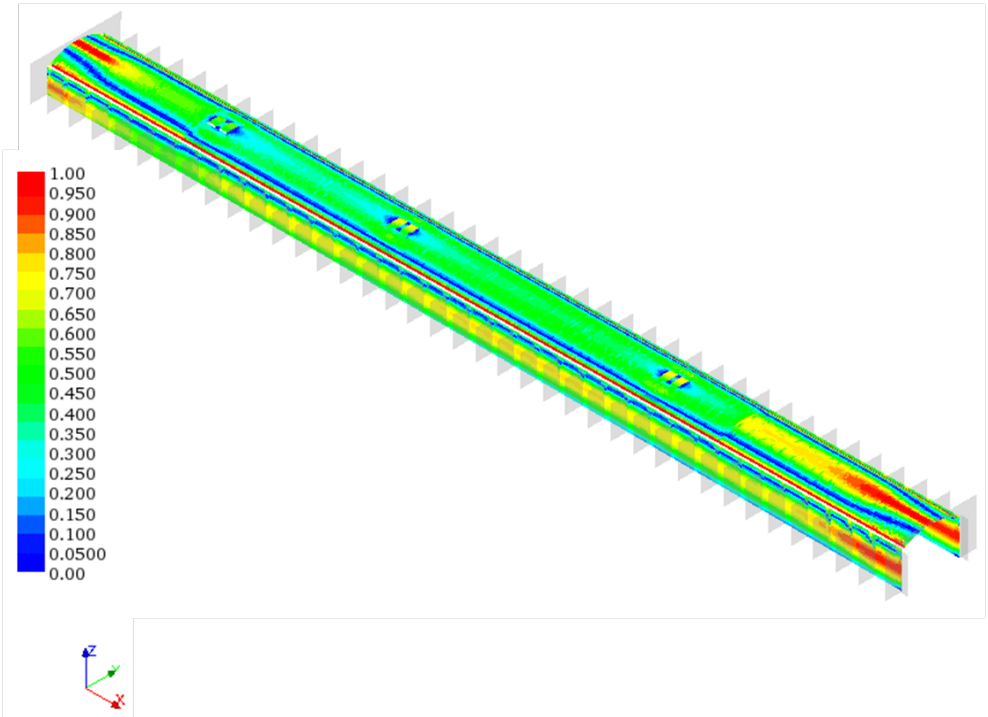

Figure 17: Case 1. Ratios $\left|\frac{M_1}{M_{1Rd}}\right|$ in the vault and $\left|\frac{M_2}{M_{2Rd}}\right|$ in the lateral walls.

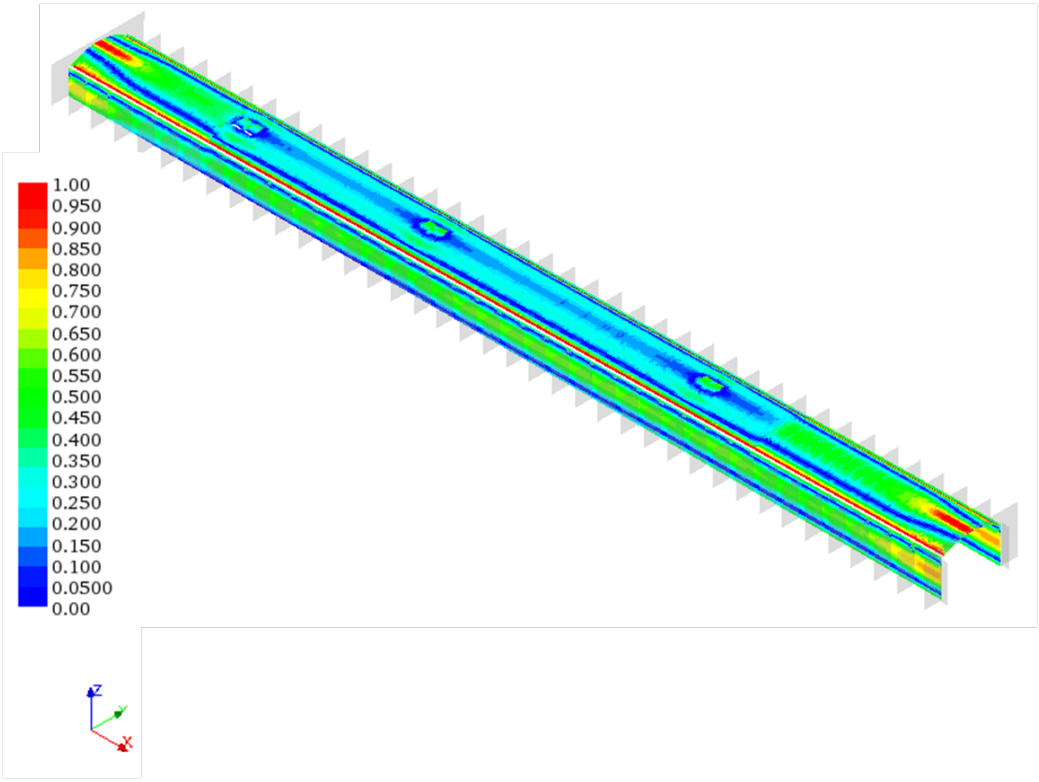

Figure 18: Case 2. Ratios $\left|\frac{M_1}{M_{1Rd}}\right|$ in the vault and $\left|\frac{M_2}{M_{2Rd}}\right|$ in the lateral walls.

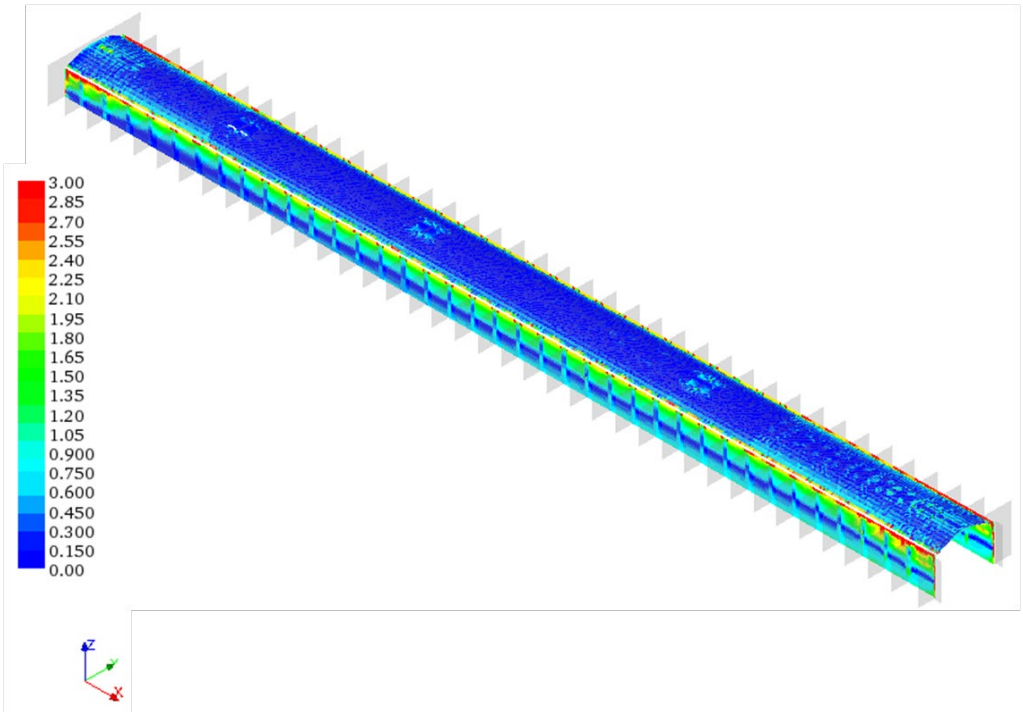

Figure 19: Case 1. Ratios $\left|\frac{T_{13}}{f_{1vd}}\right|$ in the vault and $\left|\frac{T_{23}}{f_{2vd}}\right|$ in the lateral walls.

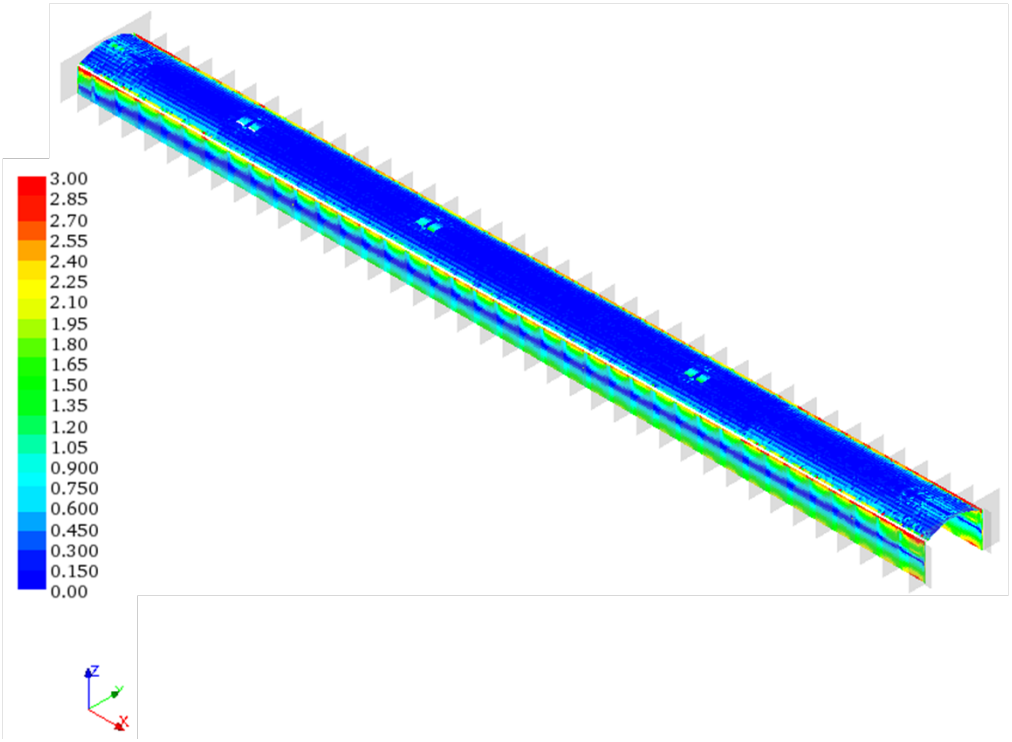

Figure 20: Case 2. Ratios $\left|\frac{T_{13}}{f_{1vd}}\right|$ in the vault and $\left|\frac{T_{23}}{f_{2vd}}\right|$ in the lateral walls.

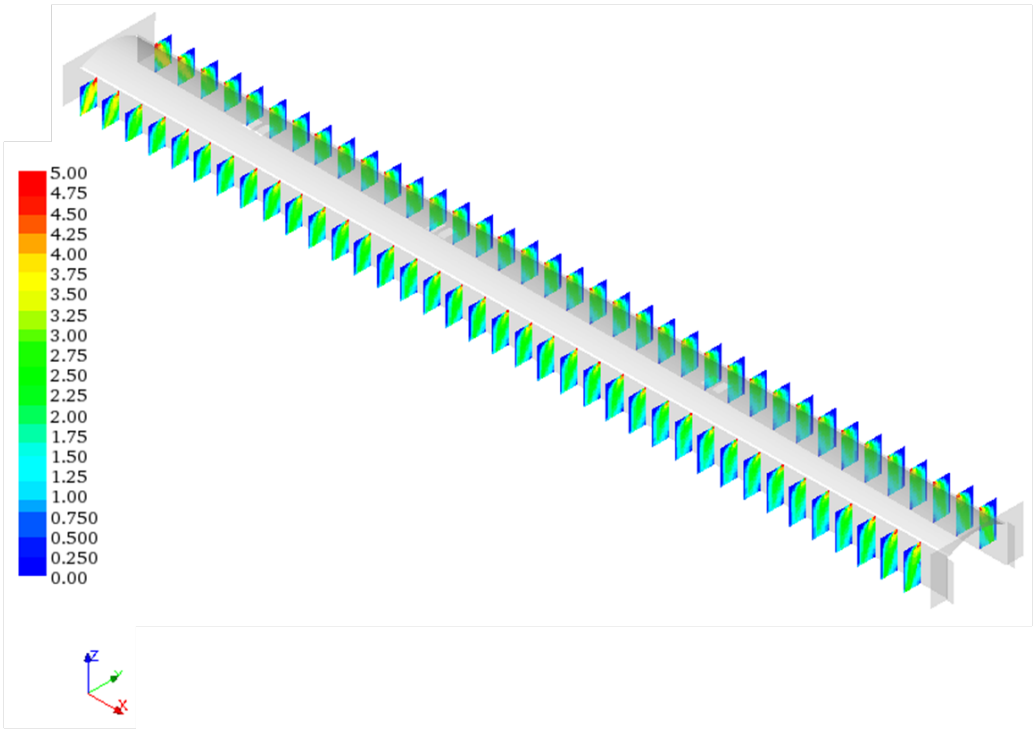

Figure 21: Case 1. Ratio $\left|\frac{T_{12}}{f_{2vd}}\right|$ in the buttresses.

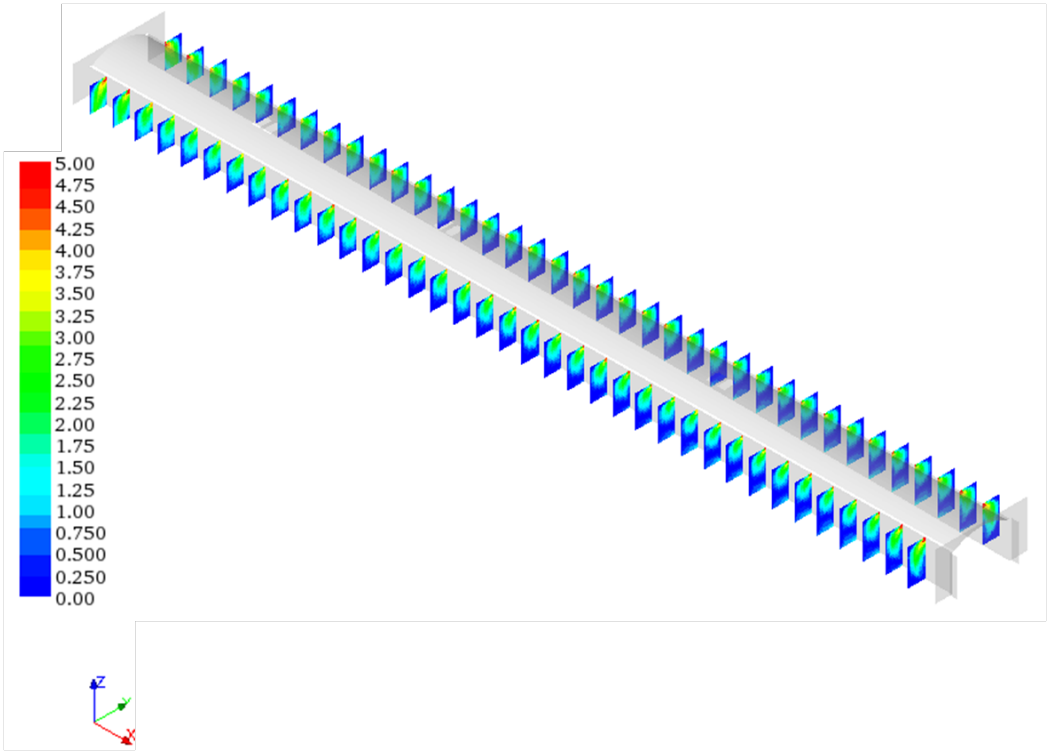

Figure 22: Case 2. Ratio $\left|\frac{T_{12}}{f_{2vd}}\right|$ in the buttresses.

4 Conclusions

The availability of ever-more sophisticated constitutive models for masonry materials, supported by increasingly powerful hardware and numerical techniques, has enabled quite realistic modelling of the mechanical behaviour of masonry constructions, whose response to tension is fundamentally different from that to compression. The constitutive equation adopted in this paper models masonry as a nonlinear elastic material with zero tensile strength and bounded compressive strength. This constitutive equation, which is known as the masonry-like (or no-tension) model, has been implemented in the finite element code NOSA-ITACA, which has been successfully applied to the static analysis of several historical masonry buildings.

Herein we have reported some results regarding application of the NOSA-ITACA code to the "Voltone", a large vaulted masonry structure located beneath the "Piazza della Repubblica" square in Livorno, Italy. Preliminary results on the static safety of the "Voltone" have been presented in [45], on which the present paper is based.

A structural analysis of the vault has been performed and the effects of the traffic loads analysed in light of current Italian regulations. These analyses have enabled calculating the stress and crack fields in the structure, also in terms of generalized stresses per unit length, and then assessing the structure's safety.

This case study, conducted in collaboration with the Municipality of Livorno, provides an opportunity to validate both the models proposed and the calculation

tool developed and highlights the key role played by numerical tools in assessing the safety of historical masonry constructions.

Acknowledgements. This research has been supported by the Region of Tuscany (project "Tools for modelling and assessing the structural behaviour of ancient constructions: the NOSA-ITACA code", PAR FAS 2007-2013). This support is gratefully acknowledged.

References

[1] International Charter for the Conservation and Restoration of Monuments and Sites, The Venice Charter 1964. 2nd International Congress of Architects and Technicians of Historic Monuments, Venice, 1964.

[2] D.V.Oliveira, P.B. Lourenco, Implementation and validation of a constitutive model for the cyclic behaviour of interface elements. Computers and Structures. 82(17–19), 1451–1461 (2004).

[3] E. Sacco, "A nonlinear homogenization procedure for periodic masonry", European Journal of Mechanics, A/Solids, 28, 209–222.

[4] J. Heyman, The masonry arch, J. Wiley &Sons, 1982.

[5] M. Gilbert, "Gross displacement mechanism analysis of masonry bridges and tunnels", in Proceedings of the 11th International Brick/Block masonry conference, Shanghai, pp. 473–482, 1997.

[6] B. Chetouane, F. Dubois, M. Vinches, C. Bohatier, "NSCD discrete element method for modelling masonry structures", International Journal for Numerical Methods in Engineering, 64, 65–94 (2005).

[7] S. Briccoli Bati, G. Ranocchiai, L. Rovero, "A micromechanical model for linear homogenization of brick masonry", Materials and Structures/Matériaux et Constructions, 32, 22-30, 1999.

[8] L. Gambarotta, S. Lagomarsino, "Damage models for the seismic response of brick masonry shear walls. part ii: the continuum model and its application", Earthquake engeneering and structural dynamics. 26, 441–462. (1997).

[9] S. Ivorra, F. J. Pallarés, "Dynamic investigation on a masonry bell tower", Engineering Structures, 28, 660-667 (2006).

[10] A. Taliercio, L. Binda, "The Basilica of San Vitale in Ravenna: Investigation on the current structural faults and their mid-term evolution", Journal of Cultural Heritage, 8, 99-118 (2007).

[11] M. Mistler, C. Butenweg, K. Meskouris, "Modelling methods of historic masonry buildings under seismic excitation", J. Seismol., 10, 497-510 (2006).

[12] M. Betti, A. Vignoli, "Numerical assessment of the static and seismic behaviour of the basilica of Santa Maria all'Impruneta (Italy)", Construction and Building Materials, 25, 4308-4324 (2011).

[13] M. Lucchesi, C. Padovani, G. Pasquinelli, N. Zani, "Masonry constructions: mechanical models and numerical applications", Series: *Lecture Notes in Applied and Computational Mechanics*, Vol. 39, Berlin Heidelberg, Springer-Verlag, 2008.

[14] K. Bernardeschi, C. Padovani, G. Pasquinelli, “Numerical modelling of the structural behaviour of Buti’s bell tower”. Journal of Cultural Heritage, 5(4), 371-378, 2004.
[15] M. Girardi, C. Padovani, A. Pagni, G. Pasquinelli, “Static analysis of masonry vaults and domes”. SMW08 - International workshop In Situ Monitoring of Monumental Surface (Firenze, 27-29 October 2008). Proceedings, pp. 335-340. P. Tiano and C. Pardini (eds.). Edifir-Edizioni Firenze, 2008.
[16] M. Girardi, C. Padovani, A. Pagni, G. Pasquinelli, “Numerical modeling of masonry towers: the case study of the Rognosa Tower in San Gimignano”, Advances and Trends in Structural Engineering, Mechanics and Computation, A. Zingoni (Editor), CRC Press/Balkema, AK Leiden, The Netherlands, 2010.
[17] M. Callieri, M. Corsini, M. Girardi, C. Padovani, A. Pagni, G. Pasquinelli and R. Scopigno, “The “Rognosa” Tower in San Gimignano: digital acquisition and structural analysis”, in B.H.V. Topping, J.M. Adam, F.J. Pallarés, R. Bru, M.L. Romero, (Editors), "Proceedings of the Tenth International Conference on Computational Structures Technology", Civil-Comp Press, Stirlingshire, UK, Paper 138, 2010. doi:10.4203/ccp.93.138
[18] http://www.nosaitaca.it/en/
[19] http://www.salome-platform.org/
[20] A. Brencich, “Assessment of Masonry Bridges: Numerical and Theoretical Approaches”, in B.H.V. Topping, L.F. Costa Neves, R.C. Barros, (Editors), "Trends in Civil and Structural Engineering Computing", Saxe-Coburg Publications, Stirlingshire, UK, Chapter 3, pp 47-76, 2009. doi:10.4203/csets.22.3
[21] A. Cavicchi, L. Gambarotta, “Lower bound limit analysis of masonry bridges including arch-fill interaction”, Engineering structures Vol. 29, pp. 3002-3104, 2007.
[22] P.J. Fanning, T.E. Boothby, “Three-dimensional modelling and full-scale testing of stone arch bridges”, Computers and Structures Vol. 97, pp. 2645-2662, 2001.
[23] D.V. Oliveira, P.B. Lourenco, C. Lemos, "Geometric issues and ultimate load capacity of masonry arch bridges from the northwest Iberian Peninsula”, Engineering Structures, Vol.32, pp. 3966-3965, 2010.
[24] LimitState: RING Manual Version 3.0f, LimitState Ltd, October 23, 2013.
[25] http://www.code-aster.org/
[26] Hinton E., Owen D. R. J., Finite Element Programming, Academic Press, 1977.
[27] P. Guidotti, M. Lucchesi, A. Pagni, G. Pasquinelli, “Elastic-Plastic Behaviour with Work Hardening: an Appropriate Model for Structural Software”. Meccanica 19, 1984.
[28] Lucchesi M., Podio-Guidugli P., “Materials with Elastic Range: a Theory with a view toward Applications. Part I”. Arch. Rat. Mech. Anal., 102, pp. 23-43, 1988.
[29] M. Lucchesi, P. Podio-Guidugli, “Materials with Elastic Range: a Theory with a view toward Applications. Part II”. Arch. Rat. Mech. Anal., 110, pp. 9-42, 1990.

[30] M. Lucchesi, D.R. Owen, P. Podio-Guidugli, “Materials with Elastic Range: a Theory with a view toward Applications. Part III. Approximate Constitutive Relations”. Arch. Rat. Mech. Anal., 117, pp. 53-96, 1992.
[31] M. Lucchesi, P. Podio-Guidugli, “Materials with Elastic Range and the Possibility of Stress Oscillations in Pure Shear”. Proc. Int. Conf. on Comp. Plasticity, Model, Software and Applications, Barcelona, 6-10 April 1987.
[32] P. Guidotti, M. Lucchesi, “A Numerical Method for Solving Boundary-Value problems in Finite Plasticity”. Meccanica, 23, pp. 43-54, 1988.
[33] G. Pasquinelli, “Simulation of Metal-Forming Processes by the Finite Element Method”. Int. J. Plasticity, 11, pp. 623-651, 1995.
[34] S. Di Pasquale, “New trends in the analysis of masonry structures”. Meccanica, 27, pp. 173-184, 1992.
[35] G. Del Piero, “Constitutive equation and compatibility of the external loads for linearly-elastic masonry-like materials”. Meccanica, 24 pp.150-162, 1989.
[36] M. Lucchesi, C. Padovani, G. Pasquinelli, “Thermodynamics of no-tension materials”. Int. J. Solids and Structures 37, pp. 6581-6604, 2000.
[37] C. Padovani, G. Pasquinelli, N. Zani, “A numerical method for solving equilibrium problems of no-tension solids subjected to thermal loads”. Comput. Methods Appl. Mech. Engrg., 190, pp. 55-73, 2000.
[38] S. Degl’Innocenti, C. Padovani, G. Pasquinelli, “Numerical methods for the dynamic analysis of masonry structures”. Structural Engineering and Mechanics, 22, pp.107-130, 2006.
[39] JK. J. Bathe, WE. L. Wilson, “Numerical methods in finite element analysis”, Prentice-Hall, Inc., Englewood Cliffs, New Jersey, 1976.
[40] M. Lucchesi, C. Padovani, G. Pasquinelli, N. Zani, “Static analysis of masonry vaults, constitutive model and numerical analysis”. Journal of Mechanics of Materials and Structures, 2, pp. 221-244, 2007.
[41] Y. Saad, “SPARSKIT: A basic tool kit for sparse matrix computations”. Technical Report, Computer Science Department, University of Minnesota, June 1994.
[42] R.B. Lehoucq, D. C. Sorensen, C. Yang, “ARPACK Users Guide: Solution of Large-Scale Eigenvalue Problems with Implicitly Restarted Arnoldi Methods”. *SIAM*, 1998.
[43] V. Binante, M. Girardi, C. Padovani, A. Pagni, G. Pasquinelli, “The NOSA-ITACA code for the modelling of the structural behaviour of historic masonry constructions”, *5th International Congress on Science and Technology for the Safeguard of Cultural Heritage in the Mediterranean Basin (Istanbul, Turkey, 22-25 November 2011)*. Proceedings, vol. II (1st part) pp. 40 - 48. Valmar, 2012.
[44] M. Girardi, M. Lucchesi, C. Padovani, B. Pintucchi, G. Pasquinelli and N. Zani, “Numerical methods for slender masonry structures: a comparative study”, in B.H.V. Topping, (Editor), "Proceedings of the Eleventh International Conference on Computational Structures Technology", Civil-Comp Press, Stirlingshire, UK, Paper 118, 2012. doi:10.4203/ccp.99.118
[45] V. Binante, S. Briccoli Bati, M. Girardi, M. Lucchesi, C. Padovani and D. Pellegrini, “A Case Study for the NOSA-ITACA Project: the “Voltone” in

Livorno”, in B.H.V. Topping, P. Iványi, (Editors), "Proceedings of the Fourteenth International Conference on Civil, Structural and Environmental Engineering Computing", Civil-Comp Press, Stirlingshire, UK, Paper 79, 2013. doi:10.4203/ccp.102.79

[46] M. Porcelli, V. Binante, M. Girardi, C. Padovani and G. Pasquinelli, “A solution procedure for constrained eigenvalues problems and its application within the structural finite-element code NOSA-ITACA”, Calcolo, Springer, online first 29 March 2014.

[47] M. Girardi, C. Padovani and G. Pasquinelli, “Numerical modelling of the static and seismic behaviour of historical buildings: the church of San Francesco in Lucca”, in B.H.V. Topping, P. Iványi, (Editors), "Proceedings of the Fourteenth International Conference on Civil, Structural and Environmental Engineering Computing", Civil-Comp Press, Stirlingshire, UK, Paper 80, 2013. doi:10.4203/ccp.102.80.

[48] M. Lucchesi, B. Pintucchi, “A numerical model for non-linear dynamic analysis of slender masonry structures”, European Journal of Mechanics A/ Solids, 26, 88-105, 2007.

[49] P. Guidotti, M. Lucchesi, A. Pagni, G. Pasquinelli, Application of Shell Theory to Structural Problem Using the Finite Element Method, Quaderni de "La Ricerca Scientifica" del CNR, 115, 1986.

[50] T. J. R Hughes., T. E. Tezduyar, “Finite elements based upon Mindlin plate theory with particular reference to the four-nodes bilinear isoparametric element”. Journal of Applied Mechanics 48, pp. 587-596, 1981.

[51] M. Lucchesi, C. Padovani and N. Zani, “Masonry like solids with bounded compressive strength ”, Int. J. Solids Structures Vol. 33, No. 14, pp. 1961-1994, Elsevier Science, 1996.

[52] C. Errico, M. Montanelli, “Il progetto del Voltone”. Private communication, 2012.

[53] V. Binante, M. Girardi, C. Padovani, G. Pasquinelli, D. Pellegrini and M. Porcelli, NOSA-ITACA 1.0 Documentation, www.nosaitaca.it/en/download, 2014.

[54] D.M. 14 gennaio 2008, Norme Tecniche per le Costruzioni, G.U. 4 febbraio 2008, n. 29.

[55] Circolare 2 febbraio 2009, n. 617, C.S.LL.PP, Istruzioni per l’applicazione delle nuove norme tecniche per le costruzioni di cui al D.M. 14 gennaio 2008.

[56] T.W. Lambe, R.V. Whitman, "Soil mechanics", John Wiley & Sons, Singapore, 1979.

[57] J.E. Bowles, “Foundation analysis and design”, McGraw-Hill, 1996.